Interpretation of the anomalous spectral dependence of the aerosol optical depth of the atmosphere. Part 1. Formal analysis of situation

S.M. Sakerin, R.F. Rakhimov, E.V. Makienko, and D.M. Kabanov

Institute of Atmospheric Optics,
Siberian Branch of the Russian Academy of Sciences, Tomsk

Received April 17, 2000

The anomalous spectral dependence of the aerosol optical depth of the atmosphere $\tau(\lambda)$ observed at intrusion of the Arctic air is discussed. This dependence is characterized by a minimum near 0.44 μm and a diffuse maximum in the range of 0.6–0.8 μm. Such a situation is quite rare for continental midlatitudes. Based on the analysis of experimental conditions and comparison with other similar data, it is supposed that the observed type of the spectral dependence $\tau(\lambda)$ can be explained by peculiarities in the microphysical composition of aerosol characteristic of clear air. The aerosol origin of the anomalous dependence $\tau(\lambda)$ is confirmed by the results of microphysical simulation that has shown the following: the diffuse maximum in the red part of the spectrum represents the optical contribution of a medium-disperse fraction of particles with the size corresponding to the first maximum of the extinction efficiency factor; the increase of $\tau(\lambda)$ in the UV region reflects the contribution of fine particles; the effect is observed at a weak influence of accumulative and coarse particles. The quantitative characteristics of the aerosol disperse structure adequate to the observed spectral dependence $\tau(\lambda)$ are presented.

Introduction

The spectral dependence of the aerosol optical depth (AOD) of the atmosphere $\tau(\lambda)$ is a result of light extinction by aerosol particles distributed nonuniformly both along the vertical direction in the atmosphere and over the size spectrum. Obviously, spatial redistribution of relatively independent elements (fractions) of the disperse structure of atmospheric haze, as well as kinetic processes controlling changes in the composition of fractions form a wide variety of the dependences $\tau(\lambda)$. At any spectral behavior $\tau(\lambda)$, the maximum aerosol turbidity in the short-wave range and the monotonic power decrease with the wavelength are common features. Situations that the dependence $\tau(\lambda)$ has a quasi-neutral shape with extremes in some wavelength ranges are more rare.

For the first time, the non-typical spectral behavior was observed by Rodionov[1] and was called the effect of anomalous transparency. Later investigations[2–7] showed that the effect is not a unique phenomenon: AOD maxima are observed in different wavelength regions and under different conditions (in mountains, Antarctic, Arctic, Eastern Europe). The common feature of most such situations is the condition of high atmospheric transparency ($\tau < 0.1$).

Different hypotheses were formulated for explaining mechanisms and causes of anomalous transparency. These hypotheses can be divided into three groups: (a) measurement instrumentation and techniques, (b) ignored absorption, and (c) aerosol nature. Different positions of $\tau(\lambda)$ maxima and different conditions of observations give grounds to doubt the validity of only one explanation common for all experiments.

Anomalous transparency of the atmosphere observed in Western Siberia under conditions of the Arctic air mass[8] is analyzed in this paper. It is shown that the observed type of the spectral behavior $\tau(\lambda)$ can be explained by peculiarities of aerosol microphysical composition characteristic of clear air conditions. In the first part of the paper, we consider only the formal approach, namely, modeling the aerosol disperse structure that is adequate to the anomalous dependence $\tau(\lambda)$ in its optical manifestation. Interpretation of the peculiarities and dynamics of the aerosol microphysical composition is considered in the second part of the paper.[15]

1. Experimental results

The issues of instrumentation and techniques for investigation of the atmospheric AOD were considered in detail in Refs. 9 and 10. Note, in particular, that observations were carried out in the spectral range from 0.35 to 1.06 μm at ten wavelengths. The photometer field of view was ~ 1.5°, and the ignored contribution of aureole adjacent illumination did not exceed 1% according to Ref. 11. The hourly mean and daily mean values of τ were used for data analysis, so the random error of measurements did not exceed ~ 0.005. The systematic error δ_τ was estimated as 0.005 to 0.01; it was principally caused by the errors in calibration and in account for gaseous constituents. In this case, the error δ_τ is more probably distributed randomly over the spectrum.

0235-6880/00/09 754-05 $02.00

Figure 1 shows the specific dependences $\tau(\lambda)$ obtained at intrusion of the Arctic air. The monotonic decrease of τ observed on July 23, 1997, was replaced with the spectral behavior with a dip near 0.44 μm and higher values in the long-wave range. The mean "depth of the anomaly" $\Delta\tau = [\tau_{0.56} - \tau_{0.44}] = 0.02$ is two to three times greater than the error in determining the AOD. The principal peculiarities of the anomalous behavior of $\tau(\lambda)$ shown by a smoothed dependence in Fig. 2*b* were kept for 2.5 days. The following transformation of the air mass manifested itself in the predominant growth of aerosol turbidity in the violet part of the spectrum, and within three to four days the spectral behavior of $\tau(\lambda)$ again became ordinary for midlatitudinal continental conditions.

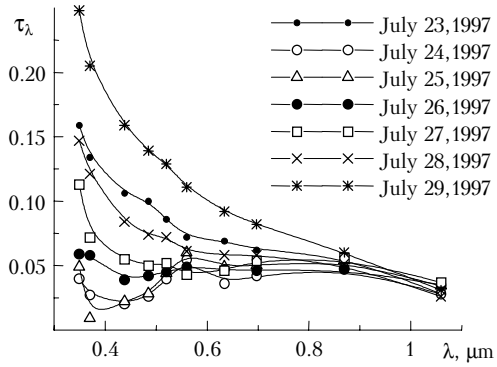

Fig. 1. Illustration of the anomalous spectral behavior $\tau(\lambda)$ and its change during the transformation of air mass.

The reliability of the extremes in $\tau(\lambda)$ in the period of the anomaly was estimated by the Student criterion in three wavelength regions: 0.35, 0.44, and 0.55–0.67 μm. The significance of the differences τ at the above-listed wavelengths was confirmed with the confidence probability more than 0.997.

The quantitative data on the AOD dynamics and meteorological parameters for the period of observations are shown in Table 1. A sharp decrease of temperature T, absolute humidity e, and the columnar water vapor W occurred in the initial period (July 24, 1997) and remained during three days. The wind velocity also was quite low. Then T, e, and W increased, but the relative humidity remained practically constant (~65%) and exceeded 70% only after July 29, i.e., neither the position of the maximum nor the condensation mechanism of its displacement toward longer waves with the increase of RH considered in Refs. 1 and 12 correspond to this case.

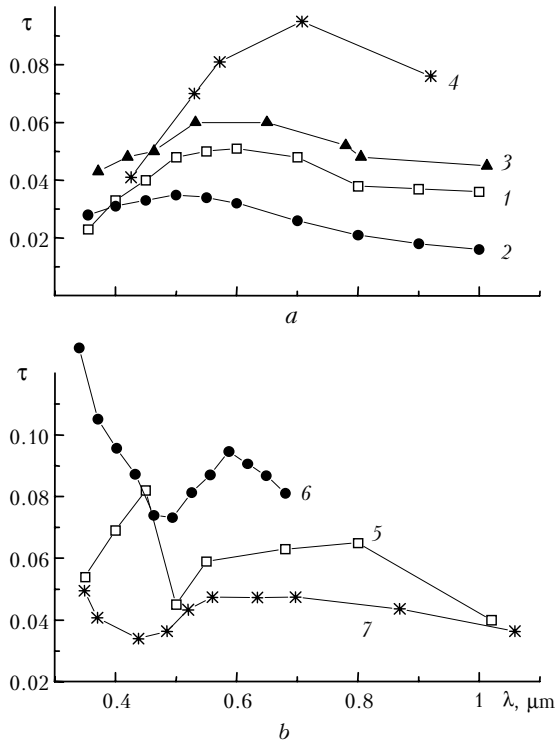

Fig. 2. Comparison of the anomalous dependences $\tau(\lambda)$ observed in different regions. Upper panel: Antarctica, station Mirnyi (Ref. 2), summer (*1*) and station Vostok, winter (*2*); Sosnovo, Leningrad Region (Ref. 3) (*3*); Ryazan (Ref. 4) (*4*). Lower panel: Abastumani, Caucasus, height of 1.6 km (Ref. 5) (*5*); SP–22 drifting station (Ref. 2) (*6*); smoothed mean dependence $\tau(\lambda)$ observed in Tomsk in July 24–26, 1997 (*7*).

Similar dependences $\tau(\lambda)$ with a diffuse maximum in the red part of the spectrum were episodically observed at intrusion of the Arctic air in the Leningrad and Ryazan Regions[3,4] (Fig. 2*a*). In our data, in contrast to Ref. 3, the maximum of $\tau(\lambda)$ did not shift toward shorter waves during the process of transformation of the air mass, but the ultraviolet maximum appeared and grew (or shifted toward longer waves). By the way, the similar UV maximum (see Fig. 2*b*) is seen in the dependences $\tau(\lambda)$ obtained in Arctic (SP–22 station,[2] 1979) and in Abastumani,[5] although the authors did not comment this fact. Judging from the long-term data,[2] the anomalous behavior of $\tau(\lambda)$ is typical for most situations in Antarctica.

Table 1. Change of $\tau(\lambda)$ and meteorological parameters of the atmosphere in the period of July 23–29, 1997 (synoptic situation: July 23 – continental moderate air, center of cyclone, cold front with rain in nighttime; July 24–26 – Arctic air, anticyclone; July 27 – warm Arctic front, continental moderate air)

Date/time of measurements	23/16:00	24/12:00	25/12:00	26/11:00	27/14:00	28/12:00	29/12:00
AOD of the atmosphere (0.52 μm)	0.086	0.040	0.044	0.045	0.052	0.072	0.129
Air temperature T, °C	27.1	18.3	17.1	16.9	21	24.7	27.4
Specific pressure of water vapor e, mbar	23.3	13.0	12.7	12.5	16.1	20	25.4
Relative humidity RH, %	65.0	62.3	65.5	64.9	64.9	64.4	69.6
Columnar water vapor W, g/cm^2	2.61	1.32	1.44	1.55	1.74	2.53	3.31
Diurnally mean wind velocity, m/s	3.1	1.7	1.6	0.8	1.3	1.7	1.9

Analysis of the conditions of the Tomsk experiment gives grounds to exclude the version of instrumental distortions[6] characteristic of more rough measurements carried out 20–30 years ago. The non-random character of observation of the anomaly also points to its reality – the principal peculiarities in the spectral behavior $\tau(\lambda)$ repeated regularly (gradually transforming) for several days. Moreover, all the considered examples for different regions (see Fig. 2) occurred not arbitrarily but only under the same conditions, namely, in the clear (Arctic or mountainous) air.

The assumption on possible appearance of selective absorption in the observed spectra $\tau(\lambda)$ is also doubtful. First, the degree of selectivity of absorption is incommensurable with more smooth dependences $\tau(\lambda)$. Second, absorption was taken into account in the LOWTRAN-7 model with control of the real variability of columnar water vapor and ozone.[9] However, one cannot exclude the presence of continuum absorption or sum contribution of very weak water vapor absorption lines.[13,14] There are no accurate data on this issue, but, according to approximate estimates, the ignored continuum absorption under conditions of low humidity does not exceed ~ 0.002. Thus, there are all grounds to explain the anomaly by peculiarities of the aerosol composition.

Anticipating microphysical modeling, let us present qualitative ideas on physical prerequisites of the anomalous dependence $\tau(\lambda)$. (Formulation of the basic hypothesis will allow us to select the domain of solution from the whole variety of aerosol disperse composition.) Principal peculiarities of the spectral behavior are the diffuse maximum in the long-wave range and the presence of the power dependence only in the violet part of the spectrum. The behavior of $\tau(\lambda)$ in the short-wave range is determined by fine particles, whose size corresponds to the range "up to the first maximum of the scattering efficiency factor." The small values of τ are indicative of the low optical activity of these particles (less than usual content of them in the atmosphere or smaller size). The diffuse maximum of τ in the long-wave range can be more likely explained by the dominant contribution of particles, whose size is in the range of the first maximum of the scattering efficiency factor, to extinction.

2. Relation between optical and microphysical characteristics

According to the Mie theory of scattering, the dependence of the atmospheric AOD on the disperse composition of aerosol has the form:

$$\tau(\lambda,r) = \int_{h=0}^{\infty} \beta_\varepsilon(h)\, \mathrm{d}h = \int_{h=0}^{\infty} \int_{r} \pi r^2 K_\varepsilon(\rho)\, f(r,h)\, \mathrm{d}h\, \mathrm{d}r, \quad (1)$$

where β_ε is the aerosol extinction coefficient, $K_\varepsilon(\rho)$ is the extinction efficiency factor depending on the complex refractive index $m = (n - i\,\kappa)$ and the Mie parameter $\rho = 2\pi r/\lambda$; r is the particle radius, $f(r, h)$ is the particle distribution function, h is the height (for simplicity, only observation in zenith is considered).

When solving the inverse problem for $\tau(\lambda)$, one usually reconstructs the integral analog of the particle distribution function

$$F_H(r) = \int f(r,h)\, \mathrm{d}h,$$

which characterizes the content of particles of different size in the atmospheric column. That is, $F_H(r)$ implicitly contains the information on the particle distribution in every layer, as well as on the peculiarities of the vertical particle distribution. Such presentation is sufficient for analysis of the total aerosol content or for comparison with other analogous distributions $F_H(r)$, but it is inconvenient in some other cases, for example, for comparison with the most numerous results of direct microphysical measurements of the "local" distribution functions $f(r)$. Let us note that the quantitative data and properties of individual fractions are determined most reliably for the surface atmospheric layer, rather than for the entire atmospheric column. Another example, where it is desirable to separate the size and height distributions, is joint analysis of the results of inversion of $\tau(\lambda)$ and the aerosol extinction coefficients $\beta_\varepsilon(\lambda)$ measured in the surface atmospheric layer.

In the general case, the aforementioned separation is difficult because of the unknown individual stratification of different-size aerosol particles. However, within relatively narrow size ranges Δr (or separate fractions) one can assume that aerosol particles have the same vertical distribution. In other words, the shape of the distribution function $f(r)$ remains the same with height, and one can separate the variables $f_i(r, h) = \mathrm{d}N(r, h)/\mathrm{d}r = f_i(r)\, g_i(h)$, where $g_i(h)$ is the vertical distribution functions for individual fractions, $\mathrm{d}N$ is the number density of aerosol particles with the radius ranging from r to $r + \mathrm{d}r$ in unit volume. In this case, $\tau(\lambda)$ can be written as a sum of the components $\tau_i(\lambda)$ caused by the effect of individual fractions:

$$\tau(\lambda) = \sum_i \tau(\lambda) = \sum_i \int_{\Delta r_i} \pi\, r^2\, K_\varepsilon\, f_i(r) \left[\int_{h=0}^{\infty} g_i(h)\, \mathrm{d}h \right] \mathrm{d}r = \sum_i H_i \int_{\Delta r_i} \pi\, r^2\, K_\varepsilon\, f_i(r)\, \mathrm{d}r, \quad (2)$$

where $H_i = \int_{h=0}^{\infty} g_i(h)\, \mathrm{d}h$ is some effective height that has the meaning of the height of a homogeneous layer for every specific fraction and profile. For example, in the simplest case of an exponential profile $g_i(h) = \exp(-\chi_i h)$ after integration we obtain $H_i = (\chi_i)^{-1}$. Equation (2) allows direct modeling, namely, synthesizing the solution $\sum_i \tau_i(\lambda)$ closest to the empirical dependence $\tau(\lambda)$ by setting different K_ε and distribution functions $F_i(r) = H_i\, f_i(r)$ for every

fraction. Besides, Eq. (2) clearly demonstrates the possibility of determining H_i if $f_i(r)$ is known and vise versa. In particular, the function $f_i(r)$ can be obtained from inversion of the aerosol extinction coefficients $\beta_\varepsilon(\lambda)$ based on the following equation:

$$\beta_\varepsilon(\lambda) = \int_{\Delta r_i} \pi r^2 K_\varepsilon f(r)\, dr. \quad (3)$$

Then, based on Eqs. (2) and (3) one can obtain the estimates of H_i that characterize the peculiarities of the vertical distribution of individual fractions.

In some cases, the function $F_H(r)$ can be presented as a product of some equivalent height H_0 common for all fractions (for example, H_0 = 1 km) and the distribution function $f^*(r)$ reduced to this height H_0. Then, instead of Eq. (2), one can write

$$\tau(\lambda) = H_0 \int_r \pi r^2 K_\varepsilon f^*(r)\, dr. \quad (4)$$

This approach gives the "distorted" idea on the particle size distribution function (in the sense that $f^*(r)$ does not characterize the particle distribution at some specific height in the atmosphere), but it is used for evaluative comparison with the known "local" functions $f(r)$. Later on the variant (4) will be used for inversion of $\tau(\lambda)$ (Ref. 15), and microphysical results will be presented in the form of the function $s(r) = dS/dr = [\pi r^2 f^*(r)]$ reduced to the height H_0 = 1 km.

3. Microphysical modeling

In the basic variant of calculations, it was supposed that the refractive index ($m = 1.45 - i\,0.005$) is constant in the analyzed spectral range, and the distribution function $f(r)$ was modeled as a superposition of logarithmically normal modes:

$$f(r) = \frac{dN}{dr} = A^{(\nu)} r^{-\nu} \sum_{i=1}^{k} M_i^{(\nu)} \exp\{-b_i [\ln(r/r_{mi}^{(\nu)})]^2\}, \quad (5)$$

where $\nu = 3$; $k = 6$; A, M_i^ν, b_i, and r_{mi}^ν are the parameters of the distribution. The distribution function included three modes in the range from 0.03 to 0.4 μm, two modes in the range from 0.4 to 1.2 μm, and one coagulation mode.

The results of modeling of $f(r)$, optical contributions of different fractions $\tau_i(\lambda)$, and their syntheses into the resulting spectral dependence are explained in Fig. 3. It is seen that the diffuse maximum in the range from 0.6 to 0.8 μm is actually caused by the prevalent contribution of particles of the medium-disperse fraction, whose size (~ 0.45–0.75 μm) corresponds to the position of the primary maximum of K_ε ($\rho \approx 5$), to aerosol extinction. The dynamics of the spectral dependence $\tau_{med}(\lambda)$ at variations of the modal radius of this fraction within 0.36 to 0.54 μm is shown in Figs. 3*d* and *a*. It is important to note that appearance of a maximum in optical data is possible if a mode width is relatively narrow. Thus, we can conclude that "optical manifestation" of the narrow medium-disperse fraction is observed in many other similar experiments.[2–5]

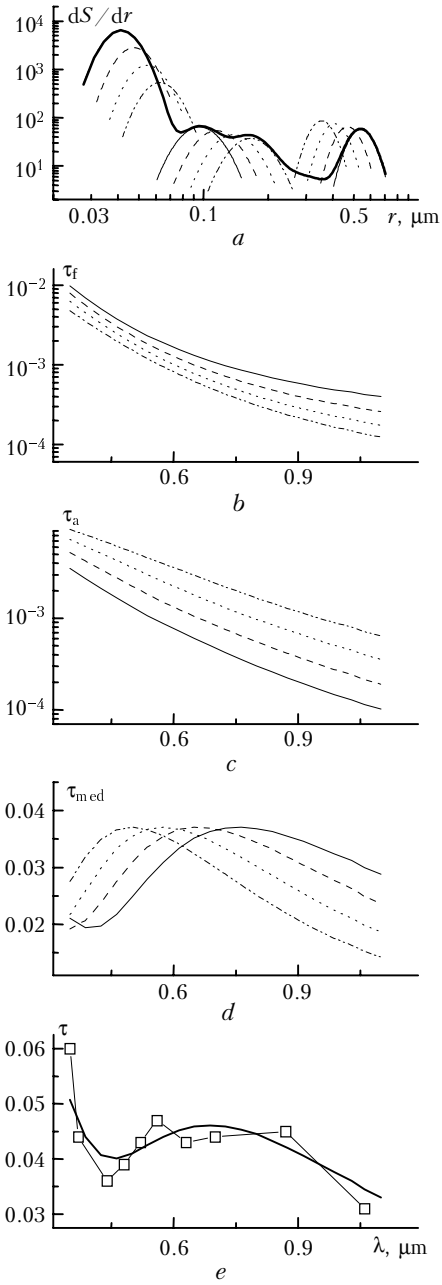

Fig. 3. Illustration of the results of modeling: model distribution $F(r)$ (*a*), spectral dependences of the optical depths of individual fractions (τ_f, τ_a, τ_{med}) (*b*, *c*, *d*); resulting calculated dependence $\tau(\lambda)$ in comparison with the experimental one (July 24, 1997) (*e*).

A qualitatively identical (Angström) spectral dependence is characteristic of particles of the fine ($r < 0.08$ μm) and accumulative (0.09 to 0.3 μm) fractions (Figs. 3*b* and *c*). However, for the minimum of $\tau(\lambda)$ in the range ~ 0.44 μm to occur, the necessary conditions are the anomalously low content of the accumulative fraction (the component τ_a) and the prevalent contribution of fine particles (the component τ_f) to formation of $\tau(\lambda)$ in the UV range. Otherwise, the spectral dependence $\tau_a(\lambda)$, as under usual condition,

"hides" specific peculiarities of manifestation of the medium-disperse fraction $\tau_{med}(\lambda)$. To keep the correspondence to optical data, the low content of the accumulative fraction should remain for two to three days with a subsequent intense increase up to the usual level. According to model estimates, the role of coarse particles is also small. Its increase leads to neutralization of the spectral behavior of AOD and the maximum (from 0.6 to 0.8 μm) becomes insignificant.

The results of modeling have shown that the best agreement with experiment is observed as the distribution functions $F_i(r)$ have the parameters presented in Table 2. In graphic representation, this case is shown in Fig. 3 by solid lines. Though modeling of other variants of the disperse structure combined with different refractive indices $m(\lambda)$ (including variable ones) affects selection of the optimal values of $F_i(r)$, but it does not lead to the principal differences in the sought result.

Table 2. Parameters of the model representation of the aerosol disperse composition corresponding to the anomalous dependence $\tau(\lambda)$

i	r_i, μm	b_i	AM_i, $\mu m^2 \cdot cm^{-3}$	N_i, cm^{-3}	S_i, $\mu m^2 \cdot cm^{-3}$	V_i, $\mu m^3 \cdot cm^{-3}$
1	0.0426	16	86.0	224	479	6.91
2	0.1000	12	2.00	111	12.9	0.438
3	0.1700	16	1.90	172	33.5	2.22
4	0.3100	1.6	0.595	16.2	10.5	1.27
5	0.5420	64	3.90	2.99	10.9	1.97
6	0.5540	64	3.90	2.86	10.9	2.01

The considered microphysical scenario is in a good agreement with the atmospheric conditions presented in Table 1. It is natural to suppose that the content of fine particles in the atmospheric column decreased sharply with income of the Arctic air. Indeed, the air in Arctic regions is characterized by a low content of both Aitken nuclei and submicron aerosol[16,17,etc] due to remoteness of these regions from aerosol sources, as well as low values of humidity, temperature, and insolation. The relatively low content of the coarse fraction is also characteristic of the Arctic air. If an air mass is transferred from the region of its formation along a short trajectory, with precipitations washing out aerosol at the leading front, the disperse composition can remain initial. Actually, at such intrusions we have the opportunity to study the aerosol optical depth of the Arctic zone.

Conclusion

Summarizing the formal analysis of the situation, we would like to note that the anomalous dependence $\tau(\lambda)$ is caused by some peculiarities in the disperse composition of particles in the size range of both primary (coarse) and secondary (fine and accumulative) aerosol.

1. The diffuse maximum of the atmospheric AOD in the red part of the spectrum is the consequence of optical manifestation of the relatively narrow medium-disperse fraction of aerosol particles, whose size ($r_m \sim 0.45$–0.55) corresponds to the first maximum of the extinction efficiency factor K_ε.

2. The effect can be observed only at the significantly low influence of particles of the accumulative ($r \sim 0.08$–0.2 μm) and coarse ($r > 1$ μm) aerosol fractions or, from the standpoint of atmospheric conditions, at weak sources of aerosol generation or a long distance from them (Antarctica, mountains, etc.). The increase of the AOD observed in some cases in the UV range reflects the contribution of fine particles ($r < 0.08$ μm).

3. The important peculiarity (for further analysis) is the two to three day delay of transformation of the spectral dependence $\tau(\lambda)$ from anomalous to the ordinary one. This delay can be explained only by conservatism of optically active fractions.

Acknowledgments

The work was supported in part by the Russian Foundation for Basic Research (Grants No. 98–05–03177–a and 00–03–32422–a).

References

1. S.F. Rodionov, *Electrophotometric Investigations of the Atmosphere over Elbrus* (Gidrometeoizdat, Leningrad, 1970), 125 pp.
2. O.D. Barteneva, N.I. Nikitinskaya, et al., *Transparency of Atmospheric Column in Visible and IR Wavelength Regions* (Gidrometeoizdat, Leningrad, 1991), 224 pp.
3. N.I. Nikitinskaya, O.D. Barteneva, and L.K. Veselova, Izv. Akad. Nauk SSSR, Fiz. Atmos. Okeana **9**, No. 4, 437–442 (1973).
4. E.E. Artemkin, in: *Atmospheric Optics* (Ryazan, 1978), pp. 3–16.
5. G.I. Kuznetsov, Izv. Akad. Nauk SSSR, Fiz. Atmos. Okeana **11**, No. 6, 647–651 (1975).
6. G.P. Gushchin, *Methods, Instruments, and Results of Measurements of Atmospheric Spectral Transparency* (Gidrometeoizdat, Leningrad, 1988), 200 pp.
7. V.L. Krauklis, G.A. Nikolskii, et al., Atm. Opt. **3**, No. 3, 201–213 (1990).
8. S.M. Sakerin and D.M. Kabanov, in: *Abstract of Reports at 5th Workshop on Siberian Aerosols* (Tomsk, 1998), pp. 38–39.
9. D.M. Kabanov and S.M. Sakerin, Atmos. Oceanic Opt. **10**, No. 8, 540–545 (1997).
10. D.M. Kabanov, S.M. Sakerin, and S.A. Turchinovich, in: *Regional Monitoring of the Atmosphere* (Tomsk, 1997), Part 2, pp. 131–145.
11. U.T. Kerimly and O.A. Kudinov, Atm. Opt. **4**, No. 2, 191–193 (1991).
12. G.V. Rosenberg, in: *Problems of Atmospheric Optics* (Leningrad State University Publishing House, Leningrad, 1979), pp. 21–24.
13. A.D. Bykov, B.A. Voronin, O.V. Naumenko, et al., Atmos. Oceanic Opt. **12**, No. 9, 755–757 (1999).
14. L.I. Nesmelova, O.B. Rodimova, and S.D. Tvorogov,. Atmos. Oceanic Opt. **10**, No. 2, 81–83 (1997).
15. R.F. Rakhimov, S.M. Sakerin, E.V. Makienko, and D.M. Kabanov, Atmos. Oceanic Opt. 13, No. 9, 759–765 (2000).
16. C. Junge, *Air Chemistry and Radioactivity* (Academic Press, New York & London, 1963).
17. K.Ya. Kondrat'ev, ed., *Aerosol and Climate* (Gidrometeoizdat, Leningrad, 1991), 542 pp.